Ultra-Low-Noise InGaAs mHEMT Technology and MMICs for Space Missions and Radio Astronomy

Fabian Thome[1], Laurenz John, Rainer Weber, Felix Heinz, Hermann Massler, Arnulf Leuther, Sébastien Chartier
Fraunhofer Institute for Applied Solid State Physics IAF, Germany
[1]Fabian.Thome@iaf.fraunhofer.de

***Abstract* — This paper demonstrates a set of wideband state-of-the-art low-noise amplifier (LNA) monolithic microwave integrated circuits (MMICs) ranging from 2 to 190 GHz. All MMICs are fabricated in a 50-nm gate-length InGaAs metamorphic high-electron-mobility transistor (mHEMT) technology. The LNAs achieve state-of-the-art noise performance for MMICs at room temperature (RT) and cryogenic conditions. The paper discusses specific design tradeoffs, such as the optimization of the input-matching network for best noise performance at RT or cryogenic condition or a lowest possible S_{11}. The discussion is exemplified with the design and measurement of three different *W*-band (75–110 GHz) LNAs. Linearity considerations are discussed based on bias-dependent single- and two-tone circuit measurements. An RF stress test and statistics over five runs and 17 wafers of the measured noise performance of W-LNA1 MMICs complete the picture of a highly reliable InGaAs mHEMT technology with state-of-the-art RT and cryogenic noise performance.**

***Keywords* — High-electron-mobility transistors (HEMTs), low-noise amplifiers (LNAs), metamorphic HEMTs (mHEMTs), millimeter wave (mmW), monolithic microwave integrated circuits (MMICs).**

I. Introduction

Cutting-edge low-noise amplifier (LNA) monolithic microwave integrated circuits (MMICs) are the key component in highly-sensitive receiver front ends. For instance, space application, such as satellite-based earth observation, commonly, demand a lowest-possible noise temperature (T_e) or noise figure (NF). Large satellite mission, such as, Meteorological Operational Satellite - Second Generation (MetOp-SG) developed by the European Space Agency and EUMETSAT are major drivers in this field. But also smaller space missions, such as, the Arctic Weather Satellite (AWS) are good examples. Recently, space missions, such as the NASA Time-Resolved Observations of Precipitation Structure and Storm Intensity with a Constellation of Smallsats (TROPICS) mission, showed impressive results based on a small CubeSat platform. Due to a considerably high effort of cryogenic cooling, a majority of space missions operate the LNAs, still today, at room temperature (RT) conditions. Only in a few examples, such as the Planck or Herschel Space Observatory, the LNAs are cooled. In contrast, radio-astronomical receivers use cooled LNAs since decades as a standard approach. Both applications, space missions and radio astronomy, are main drivers for further technology and circuit developments for improving the noise performance of sensitive receiver systems at room and cryogenic temperatures at microwave, millimeter-wave, and even submillimeter-wave frequencies.

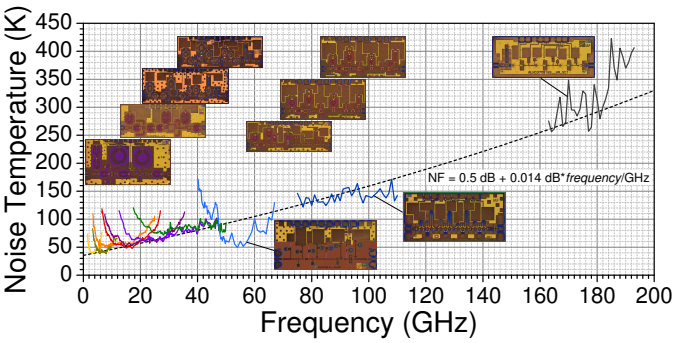

Fig. 1. Summary of the measured room-temperature T_e of the presented LNA MMICs realized in our 50-nm InGaAs mHEMT technology in the frequency range from 2 to 190 GHz. The black dashed line illustrates a trend line.

Today, the best transistor-based noise performance is achieved by InGaAs high-electron-mobility transistors (HEMTs), which, in general, exist in two types. First, so-called InP HEMTs [1]–[5] that are grown directly on native InP substrates and, second, metamorphic HEMTs (mHEMTs) [6]–[9] where a metamorphic buffer adapts the lattice constant of the GaAs substrates to the value of InP. The active layers can be nominally identical.

This work presents a set of wideband LNA MMICs achieving state-of-the-art noise performance for operating frequencies of up to 190 GHz (please see Fig. 1). The MMICs are fabricated in the Fraunhofer IAF 50-nm InGaAs mHEMT technology. The paper is organized as follows: Section II summarizes the used 50-nm InGaAs mHEMT technology. Section III discusses important design aspects for a cutting-edge LNA performance. Furthermore, the impact of different optimization goals for the input matching network (IMN) is discussed based on three *W*-band LNAs. In Section IV, the measurements of the presented MMICs are discussed. An investigation of the statistics of the measured T_e of W-LNA1 is shown and linearity measurements as well as an RF stress test conclude the measurements.

II. 50-nm InGaAs mHEMT Technology

This work is based on our in-house 50-nm gate-length mHEMT technology. The 2-D electron gas is confined in an $In_{0.8}Ga_{0.2}As$ channel with $In_{0.52}Al_{0.48}As$ barrier layers in a double heterostructure. The active layers are grown on 100-mm GaAs substrates. The T-gate is encapsulated in benzocyclobutene (BCB) and a 250-nm-thick SiN layer. The process

Table 1. Summary of the Measured Performance of the Presented LNA MMICs

Circuit	BW (GHz)	T_a (K)	P_{dc} (mW)	Chip Size (mm^2)	S_{11} (dB)	Gain (dB)	NF (dB)	T_e (K)
S-LNA	2–4	297	39.6	2.75 × 1.5	<−6.7	33.9–36.7	0.6–0.7 (av 0.6)	40–49 (av 42)
	2–5				<−5	29.1–36.7	0.6–0.7 (av 0.6)	40–51 (av 43)
C-LNA [10]	4–8	297	24.8	2.5 × 1	<−2.4	26.8–32.4	0.5–0.8 (av 0.6)	38–62 (av 44)
IF-LNA	4–20	297	90.1	3 × 1.25	<−4.5	34.5–41.3	0.6–1.1 (av 0.8)	46–84 (av 58)
Ku-LNA [9]	12.4–18	297	154.9	2.5 × 1	<−8.4	39.3–41.1	0.7–0.8 (av 0.7)	48–57 (av 52)
	8–20				<−8	38.3–41.8	0.7–1 (av 0.8)	48–77 (av 57)
	8–18	10	24.4		n/a	38.5–40.5	0.05–0.08 (av 0.06)	3.3–5.6 (av 4.2)
K-LNA	18–26.5	297	71.8	2.75 × 1	<−7.4	34.7–38	0.8–0.9 (av 0.8)	56–66 (av 62)
	10–30				<−3.1	30.7–38	0.7–1 (av 0.8)	52–78 (av 63)
Ka-LNA	26.5–40	297	31.3	2 × 1	<−5.3	30.2–31.8	0.8–1.1 (av 1)	62–86 (av 76)
	15–48				<−3.2	28.9–35.8	0.8–1.3 (av 1)	60–102 (av 75)
Q-LNA	33–50	297	27.9	2 × 1	<−4	29.7–31.4	1–1.3 (av 1.1)	77–101 (av 87)
	20–50					27.9–31.7	1–1.3 (av 1.1)	72–101 (av 85)
V-LNA	48–58	297	39.6	2 × 1	<−9.5	31.6–34.6	0.7–1 (av 0.8)	49–75 (av 61)
	48–64					28.9–34.6	0.7–1.3 (av 0.9)	49–101 (av 68)
W-LNA1 [11]	75–110	297	25.5	1.5 × 0.75	<−10	24.3–28.5	1.5–2 (av 1.7)	122–171 (av 141)
W-LNA2	75–108	297	25.5	1.5 × 0.75	<−15	20.8–27.4	1.7–2.2 (av 1.9)	141–196 (av 157)
W-LNA3 [8]	75–108	297	28.7	1.5 × 1	−9	21.4–26	1.8–2.5 (av 2.1)	151–228 (av 177)
	67–116	15	14.6		n/a	19.9–28.9	0.2–0.4 (av 0.31)	13.6–27.9 (av 21.4)
G-LNA	163–190	297	23	1.75 × 0.75	<−5.9	25.4–32.9	2.7–3.9 (av 3.3)	256–423 (av 315)

features two Au-based interconnect metallization layers. The top galvanic layer can be realized in air-bridge technology. After finishing the front-side process, the wafers are thinned to a thickness of 50 μm. At the end, through-substrate vias and a backside metallization is defined.

III. LNA Design and Tradeoffs

All presented MMICs are designed and fabricated in the aforementioned 50-nm mHEMT technology addressing different frequency bands. A summary of the presented MMICs is listed in Table 1. The LNAs can be grouped in three categories. First, LNAs up to operating frequencies of 50 GHz (including Q-LNA), are based on common-source (CS) stages and the matching networks, especially the IMN, are based on planar lumped components, such as spiral inductors. Especially the use of spiral inductors is a key for a wideband performance. Compared to transmission lines with a high characteristic impedance, low-loss matching networks can be realized by spiral inductors. The relatively low parasitic capacitance of air-bridge inductors is a key to achieve a considerably large bandwidth (BW) paired with low losses. The resulting high frequency of the first resonance allows for wideband performance up to high frequencies. However with increasing operating frequency, the size of the spiral inductors needs to be shrunk. At frequencies above approximately 50 GHz, the inductors would have to be so small that a realization is either impossible or not possible without significant performance losses.

Second, LNAs targeting frequencies above 50 GHz are based on networks using transmission lines. The LNAs up to W-band are still based on CS stages. As discussed in [12], the source, gate, and drain stubs feature transmission lines with a high characteristic impedance. Furthermore, the drain stubs are connected close to the HEMT in order to enhance the BW.

Third, at high frequencies, the transistor gain decreases. Therefore, the G-LNA (160 to 190 GHz) uses three cascode stages in order to increase the gain per stage. The IMN of the G-LNA is realized by a grounded coplanar waveguide with a ground-to-ground (G2G) spacing of 50 μm for low losses.

For frequencies of below 10 GHz, the gain per stage is high enough so that a two-stage design is feasible while still achieving approximately 30 dB of LNA gain. The MMICs between 10–50 GHz use three stages, whereas the LNAs in V- and W-band contain four stages. At least in the first stage, all LNAs use the well-established inductive source degeneration to simultaneously improve noise and power matching.

In the last part of this section, the tradeoffs when designing the IMN are discussed. It is commonly known that one has to trade the input power matching against the noise performance. To quantify this tradeoff, two W-band LNAs are compared. W-LNA1 builds on previous research of [11] and is optimized for a lowest possible T_e at RT. The simulated and measured performance is shown in Fig. 2(a). The simulations are based on a temperature dependent and scalable HEMT model [13]. S_{11} is predicted with a value of better than −10 dB. W-LNA2 targets a better S_{11} of below −15 dB, which is achieved by minor modifications of the IMN. This ensures that other circuit parameters remain comparable. The length of W-LNA2's gate stub has been decreased from 80 to 65 μm compared to W-LNA1. Furthermore, the length of the source line has been increased from 60 to 80 μm to achieve the desired S_{11}. However, the increased source degeneration leads to a reduced gain and by that, a negative impact on T_e of W-LNA2 is expected. The difference of the IMN optimized for cryogenic or RT conditions concerns mainly the noise matching. The source impedance for lowest noise changes and the matching has to be adopted for cryogenic conditions since various circuit

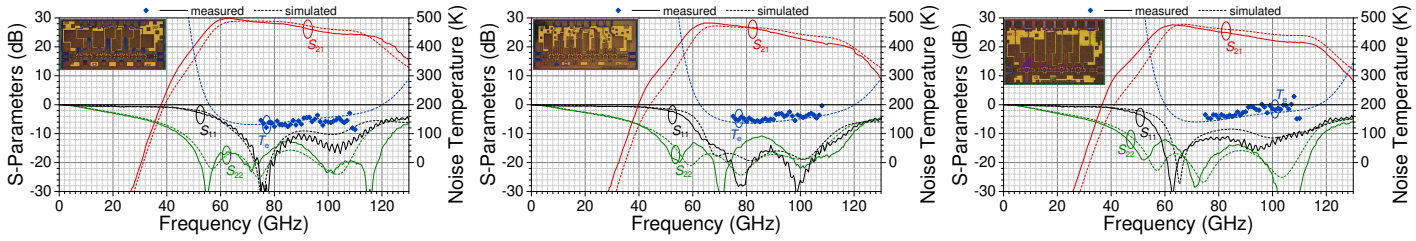

(a) (b) (c)

Fig. 2. Measured and simulated RT S-parameters and T_e of the presented W-band LNAs optimized for different design targets. (a) W-LNA1 is optimized for a best-achievable T_e at RT, whereas in (b) W-LNA2 is designed for an improved S_{11}. (c) W-LNA3 is optimized for cryogenic operation. The LNAs are operated for an RT-noise-optimized bias point of $V_{ds} = 0.6\,V$ and a drain current of 200 mA/mm.

parameters change, such as the HEMT bias or the resistance of metals. Similar to W-LNA2, the IMN optimization for W-LNA3 is mainly done by adjusting the length of the gate stub and the source line at the first transistor. The length of the gate stub is decreased from 80 to 75 μm and the source line is considerably increased from 60 to 130 μm. W-LNA1 is matched for best noise at RT while W-LNA3 is optimized for cryogenic temperatures. Consequently, the T_e is degraded for the temperature that has not been targeted. As a result, the improvement of T_e when cooling the LNA is considerably larger for the cryogenic optimized case (W-LNA3) since the T_e at RT is higher compared to the RT optimized W-LNA1. Based on simulations, the expected T_e (averaged over the entire W-band) for W-LNA1 and W-LNA3 at RT is 148.8 and 162.5 K, which reduces to 21 and 19.4 K, respectively, when cooled to 15 K. This means by optimizing the IMN, the expected T_e at cryogenic temperatures is about 8 % better for the cryogenic-optimized W-LNA3, while having a penalty at RT of more than 9 %. Consequently, the T_e improvement for W-LNA1 and W-LNA3 is approximately 7 and 8.4, respectively.

IV. Measurement Results

The measured performance of all presented LNA MMICs is summarized in Table 1 and the measured T_e is shown together with the corresponding chip photos of the fabricated MMICs in Fig. 1. All MMICs are biased for optimum noise. Up to 50 GHz, the MMICs are characterized using a Keysight PNA-X setup with integrated noise receiver using a vector-corrected cold-source method [14]. Above, commercially-available waveguide noise sources are used in combination with downconverter modules and a noise figure analyzer operating at intermediate frequencies. In Fig. 1, the black dashed line illustrates a fitted trend line. The trend line indicates an offset of about 35 K or 0.5 dB, which can be attributed to, e.g., losses in the on-chip IMN. Furthermore, a frequency-depending part with a slope of 0.014 dB per additional gigahertz adds to the offset.

In Fig. 2, the presented measurements resume the discussion on the IMN tradeoff for different design targets. Fig. 2(a) shows the performance of the RT-noise-optimized W-LNA1. The measured T_e is between 122–171 K (NF: 1.5–2 dB) with an average of 141 K (1.7 dB). The S_{11} is better than −10 dB

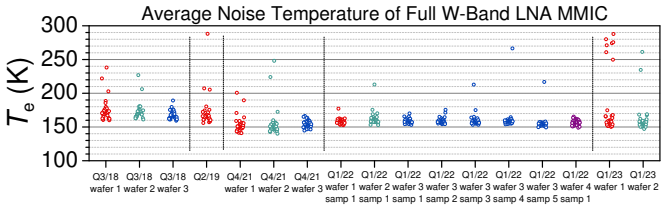

Fig. 3. Measured statistics of the average T_e (weighted average from 75 to 110 GHz) over five runs and 17 wafers during the last four years showing low inter and intra run variation. Each dot is the average T_e of a W-LNA1 MMIC as part of a full wafer mapping.

over the entire W-band. Fig. 2(b) presents the measurements of W-LNA2. As intended, the S_{11} is improved to values of below −15 dB. T_e is slightly increased by approximately 11 % (NF increase: 0.2 dB), which has been expected. The RT performance of the cryogenic-optimized W-LNA3 is depicted in Fig. 2(c). The average T_e (177 K) at RT is approximately 25 % higher, which is slightly more than simulated, but strengthens even more the hypothesis of the need for an application-dependent optimization of the IMN.

Fig. 3 shows some statistics of the achievable T_e within a wafer, between different wafers of a wafer batch, and between different runs. The variation of T_e within a wafer is approximately below 10 % for at least 75 % of the available cells. For a majority of wafers, the spread is even less for a higher yield. The wafer-to-wafer variation shows comparable values as the intra-wafer variation.

For some applications, an LNA has to withstand for a short time a considerably high input power (P_{in}), e.g., when a signal of a transmitter is partly reflected to the receiver. Therefore, an RF stress test was performed at 85 GHz, where a P_{in} of 0 dBm was provided to the RF input of a sample of W-LNA1 for more than 24 h. A P_{in} of 0 dBm corresponds to a gain compression of 24 dB. For the test, a diced MMIC of W-LNA1 was glued with a silver-filled epoxy on a brass carrier and contacted with on-wafer probes. Before and after the RF stress test, T_e of the LNA was measured. The measurement results are compared in Fig. 4. The difference of the average T_e is approximately 2 %. Considering the repeatability of noise measurements in W-band, one can conclude that the difference is negligible.

To complete the measurements, single- and two-tone lin-

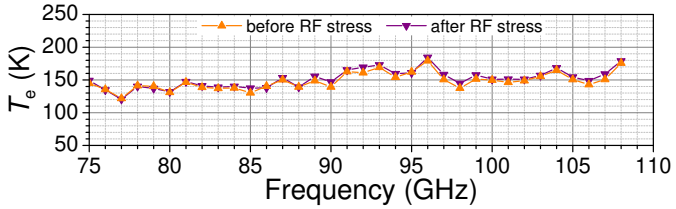

Fig. 4. Measured T_e before and after stressing a sample of W-LNA1 with a P_{in} of 0 dBm for more than 24 h.

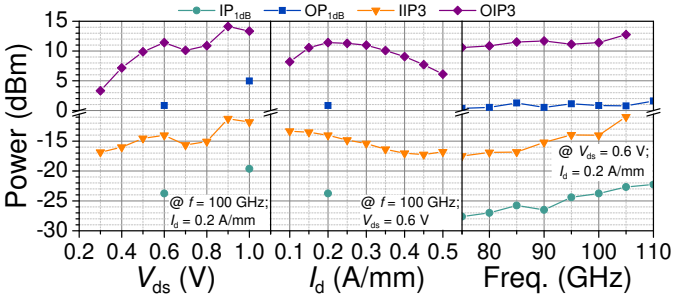

Fig. 5. Measured P_{in} and P_{out} at 1-dB gain compression and input- and output-referred third-order intercept point versus (a) V_{ds}, (b) I_d, and (c) operating frequency of W-LNA1.

earity measurements are performed in W-band for different bias conditions of W-LNA1. It is interesting to observe that related to OIP3, the optimum drain current (I_d) is 200 mA/mm, which is also the optimum for T_e [11]. When increasing the drain voltage (V_{ds}) from the noise optimum ($V_{ds} = 0.6$ V) to 1 V, the 1-dB gain compression improves by approximately 4 dB ($OP_{1\,dB}$ from 0.8 to 5 dBm). This is in line with load-pull measurements in W-band on device level where the output power (P_{out}) density at $P_{1\,dB}$ for a V_{ds} of 0.6 and 1 V is 30 and 80 mW/mm, respectively.

V. Conclusion

This paper presents a set of LNA MMICs demonstrating state-of-the-art noise performance for MMICs over a frequency range from 2 to 190 GHz. The LNAs are fabricated in the Fraunhofer IAF 50-nm InGaAs mHEMT technology. Wafer mappings of T_e (17 wafers fabricated in five different batches) of a *W*-band LNA highlight a remarkable yield and reproducibility of such a cutting-edge MMIC. A record T_e of the *W*-band LNA of below 171 K (2 dB) over the entire *W*-band with an average T_e of 141 K (NF = 1.7 dB) is achieved. Further LNA MMICs at different frequency bands confirm the state-of-the-art noise performance. Furthermore, an RF stress test with a P_{in} of 0 dBm over 24 h results in no major change in noise performance. This demonstrates the robustness of such a high-speed and noise-optimized HEMT technology. In combination with single- and two-tone linearity measurements, the presented technology and MMICs provide an appealing performance for space mission, such as earth observation or communication satellites. In addition to the excellent RT T_e, the technology exhibits as well state-of-the-art cryogenic noise temperatures with, e.g., a demonstrated T_e in *W*-band of four times the quantum limit [8].

Acknowledgment

The authors thank the colleagues in the epitaxy and technology departments of the Fraunhofer IAF for their excellent contributions during epitaxial growth and wafer processing. Some of the data samples have been obtained as part of the LNA development for ESA's Arctic Weather Satellite mission. The authors thank Omnisys Instruments AB for their support during the LNA-MMIC development. Furthermore, the project has received partly funding from the European Union's Horizon 2020 research and innovation programme under Grant agreement number 871764.

References

[1] W. Deal, X. B. Mei, K. M. K. H. Leong, V. Radisic, S. Sarkozy, and R. Lai, "THz Monolithic Integrated Circuits Using InP High Electron Mobility Transistors," *IEEE Trans. THz Sci. Technol.*, vol. 1, no. 1, pp. 25–32, Sep. 2011, doi: 10.1109/TTHZ.2011.2159539.

[2] J. Schleeh *et al.*, "Ultralow-Power Cryogenic InP HEMT With Minimum Noise Temperature of 1 K at 6 GHz," *IEEE Electron Device Lett.*, vol. 33, no. 5, pp. 664–666, May 2012, doi: 10.1109/LED.2012.2187422.

[3] D. Cuadrado-Calle *et al.*, "Broadband MMIC LNAs for ALMA Band 2+3 With Noise Temperature Below 28 K," *IEEE Trans. Microw. Theory Techn.*, vol. 65, no. 5, pp. 1589–1597, May 2017, doi: 10.1109/TMTT.2016.2639018.

[4] N. Estella, L. Bui, E. Camargo, and J. Schellenberg, "35nm InP HEMT LNAs at E/W-Band Frequencies," in *IEEE Compound Semicond. Integr. Circuits Symp. Dig.*, Oct. 2016, pp. 1–3, doi: 10.1109/CSICS.2016.7751007.

[5] Y. Tang *et al.*, "Cryogenic W-band LNA for ALMA band 2+3 with average noise temperature of 24 K," in *IEEE MTT-S Int. Microw. Symp. Dig.*, Jun. 2017, pp. 176–179, doi: 10.1109/MWSYM.2017.8058981.

[6] A. Leuther, A. Tessmann, H. Massler, R. Aidam, M. Schlechtweg, and O. Ambacher, "450 GHz Amplifier MMIC in 50 nm Metamorphic HEMT Technology," in *Proc. Int. Conf. Indium Phosphide Rel. Mater.*, Aug. 2012, pp. 229–232, doi: 10.1109/ICIPRM.2012.6403365.

[7] P. Smith *et al.*, "A 50nm MHEMT millimeter-wave MMIC LNA with wideband noise and gain performance," in *IEEE MTT-S Int. Microw. Symp. Dig.*, Jun. 2014, pp. 1–4, doi: 10.1109/MWSYM.2014.6848288.

[8] F. Thome, F. Schäfer, S. Türk, P. Yagoubov, and A. Leuther, "A 67–116-GHz Cryogenic Low-Noise Amplifier in a 50-nm InGaAs Metamorphic HEMT Technology," *IEEE Microw. Compon. Lett.*, vol. 32, no. 5, pp. 430–433, May 2022, doi: 10.1109/LMWC.2021.3134462.

[9] F. Heinz, F. Thome, A. Leuther, and O. Ambacher, "A 50-nm Gate-Length Metamorphic HEMT Technology Optimized for Cryogenic Ultra-Low-Noise Operation," *IEEE Trans. Microw. Theory Techn.*, vol. 69, no. 8, pp. 3896–3907, Aug. 2021, doi: 10.1109/TMTT.2021.3081710.

[10] F. Heinz, F. Thome, A. Leuther, and O. Ambacher, "C-Band Low-Noise Amplifier MMIC with an Average Noise Temperature of 44.5 K and 24.8 mW Power Consumption," in *Proc. Eur. Microw. Integr. Circuits Conf.*, Apr. 2022, pp. 144–147, doi: 10.23919/EuMIC50153.2022.9783784.

[11] F. Thome, A. Leuther, F. Heinz, and O. Ambacher, "W-Band LNA MMICs Based on a Noise-Optimized 50-nm Gate-Length Metamorphic HEMT Technology," in *IEEE MTT-S Int. Microw. Symp. Dig.*, Jun. 2019, pp. 168–171, doi: 10.1109/MWSYM.2019.8700792.

[12] F. Thome, A. Leuther, H. Massler, M. Schlechtweg, and O. Ambacher, "Comparison of a 35-nm and a 50-nm Gate-Length Metamorphic HEMT Technology for Millimeter-Wave Low-Noise Amplifier MMICs," in *IEEE MTT-S Int. Microw. Symp. Dig.*, Jun. 2017, pp. 752–755, doi: 10.1109/MWSYM.2017.8058685.

[13] F. Heinz, F. Thome, D. Schwantuschke, A. Leuther, and O. Ambacher, "A Scalable Small-Signal and Noise Model for High-Electron-Mobility Transistors Working Down to Cryogenic Temperatures," *IEEE Trans. Microw. Theory Techn.*, vol. 70, no. 2, pp. 1097–1110, Feb. 2022, doi: 10.1109/TMTT.2021.3123647.

[14] Keysight Technologies, Inc., "High-Accuracy Noise Figure Measurements Using the PNA-X Series Network Analyzer (AN 1408-20)," Aug. 2014. [Online]. Available: https://literature.cdn.keysight.com/litweb/pdf/5990-5800EN.pdf